Heliyon 10 (2024) e33121

Contents lists available at ScienceDirect

Heliyon

journal homepage: www.cell.com/heliyon

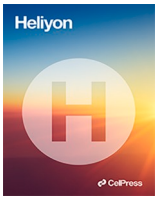

Research article

Production of low-sulfur fuels from catalytic pyrolysis of waste tires using formulated red mud catalyst

Foster A. Agblevor [a,*], Oleksandr Hietsoi [b], Hossein Jahromi [c], Hamza Abdellaoui [d]

[a] USTAR Bioenergy Center, Biological Engineering Department, Utah State University, Logan, UT, USA
[b] Chemistry Department, Middle Tennessee State University, Murfreesboro, TN, USA
[c] Biosystems Engineering Department, Auburn University, Auburn, AL, USA
[d] Biological Engineering Department, Utah State University, Logan, UT, USA

ARTICLE INFO

Keywords:
Waste tires
Catalytic pyrolysis
Red mud
Pyrolysis oils
Sulfur

ABSTRACT

Waste tires (WT) are produced in millions of tons per annum and their safe disposal is always a major environmental challenge because of fire hazards and the increasing cost of landfills. WT has high organic matter content that can be converted into fuels and chemicals if suitable technologies can be developed. Herein we report the *in situ* catalytic pyrolysis of WT using formulated red mud catalyst to produce low sulfur fuel that can be fractionated or can be used without fractionation. The *in situ* catalytic pyrolysis was conducted at 450–550 °C using formulated red mud catalyst. The yield of pyrolysis liquids ranged from 35 to 40 wt%. The liquid was very rich in limonene and long chain aliphatic hydrocarbons. The catalyst was effective in removing the sulfur compounds in the oil through reactive adsorption desulfurization mechanism. The sulfur species reacted with hematite, calcite, sodium hydroxide, and zinc oxide to form sulfides and were retained in the catalyst. The minimum sulfur content of the catalytic pyrolysis oil was 0.38 wt%. After catalyst regeneration in air through combustion, the catalyst activity was restored, and the catalyst was reused.

1. Introduction

Energy production and utilization is one of the main drivers of human civilization and until we master how to produce it sustainably and distribute it efficiently, human civilization will always be threatened for survival. Currently, there are millions of tons of organic materials, which are classified as waste because we do not know how to efficiently utilize them to benefit humankind. A classic example is waste tires (WT) which are ubiquitous in every country. Disposal of these WT are increasingly becoming a challenge especially in tropical countries where they can potentially become disease vectors such as malaria and zika virus because they become breeding grounds for mosquitoes and other pests. The traditional disposal methods such as land filling, road applications, playground applications, direct pyrolysis to produce high sulfur heating fuels, and combustion as tire-derived fuels (TDF) are becoming inadequate because of pollution problems associated with them. About 300 million tires are disposed of annually in landfills, combustion, and other disposal methods in the USA [1].

WT are composed of rubber/elastomers (natural and synthetic), steel wires, carbon black, silica, textiles, vulcanizer agents (sulfur, zinc oxide, and stearic acid), and additives (clay fillers, oil, and other agents) [2]. These materials occur in different proportions in

* Corresponding author.
E-mail address: foster.agblevor@usu.edu (F.A. Agblevor).

https://doi.org/10.1016/j.heliyon.2024.e33121
Received 23 September 2023; Received in revised form 5 June 2024; Accepted 14 June 2024
Available online 19 June 2024

various tires. The compositions may vary slightly, but in general they all contain different proportions of these materials. Typical compositions of waste tires are shown in Table 1 [2].

The organic fractions of the tires, such as rubber/elastomers and textiles can be converted into liquid and gaseous fuels using either pyrolysis or gasification technologies. Gasification of WT produces high energy gases containing significant amounts of sulfur compounds that must be removed before utilization. The sulfur removal operations tend to increase the production cost of the syngas and therefore makes it less competitive with natural gas.

The WT carbonaceous fraction can also be combusted as TDF for heat and power generation. TDF is the oldest and most developed market in the USA [3]. TDF is used in cement kilns, pulp and paper mills, electric utilities, and other applications [3]. However, this application produces considerable amounts of SOx, NOx, and heavy metals that require pollution abatement equipment to reduce harmful emissions [3].

Pyrolysis technology can potentially be used to extract energy from WT under suitable reaction conditions [4–10]. Pyrolysis is a thermochemical decomposition of organic material at elevated temperatures in the absence of oxygen. WT pyrolysis involves the thermal decomposition of tire shreds into low molecular weight products in an inert atmosphere. The three main products obtained from WT pyrolysis are: char, oil, and gas. The main gas components of WT pyrolysis are H_2, C_1–C_4 hydrocarbons, CO_2, CO, and H_2S. The gas fraction can be used as fuel in the pyrolysis process. Tire pyrolysis oil is chemically complex containing aliphatic, aromatic, heteroatom, and polar fractions. Its high calorific value can be used for production of high-quality fuels [11,12].

The main barrier for its direct fuel utilization is the high sulfur content [12–14]. WT pyrolysis oils contain 1.00–1.35 wt% sulfur [15], which makes them unsuitable for transportation fuels where the sulfur content is typically below 0.05 wt% [16]. The sulfur content of these oils can also be reduced through various sweetening or desulfurization processes, but these unit operations increase the cost of fuel and thus make them uncompetitive relative to petroleum derived heating fuels. Thus, the conversion of WT to energy must incorporate desulfurization strategy in order to meet environmental pollution standards [16,17] and also reduce the conversion cost by incorporating sulfur reducing units in the pyrolysis process through such processes as catalytic pyrolysis.

This paper is focused on the catalytic pyrolysis of WT and therefore more attention is paid to this literature rather than the entire tire pyrolysis literature. Catalytic pyrolysis of WT, just like catalytic pyrolysis of any biomass, is aimed at improving the pyrolysis oil quality for higher value applications. The catalytic pyrolysis process involves both *ex situ* and *in situ* approaches. Most WT catalytic pyrolysis studies have focused on zeolite catalysts because of their high acidity and shape-selectivity due to different pore sizes. Thus, ZSM-5, HY, Hbeta, HMOR, SAPO-11 have all been investigated by various researchers to improve fuel quality. An extensive review of catalytic pyrolysis of WT has been reported, which showed WT pyrolysis oil yields ranged from 14.8 to 56 wt% depending on the catalyst, reaction temperature, and reactor type [18]. In addition to zeolites, some basic catalysts such as CaO, MgO, FeO have been investigated for both catalytic pyrolysis and *ex situ* desulfurization of the WT pyrolysis oils and were reported to be effective [19]. William and Brindle [20] reported the selective production of benzene, toluene, and xylenes (BTX) using Y zeolites and ZSM-5 catalysts. Kar [21] reported increased yield of liquid fraction when expanded perlite catalyst was used to pyrolyze WT. Zhang et al. [22] used NaOH additive for the pyrolysis of WT and reported lower pyrolysis temperature relative to thermal pyrolysis without any additive. Olazar et al. [23] studied the effect of catalyst on the composition of tire pyrolysis products and observed that both HY and HZSM-5 strongly influenced the pyrolysis products. HZSM-5 promoted the formation of olefins, produced more gaseous products, and decreased the molecular weight of the liquid products because of increased cracking. The HY zeolite, because of larger pore size was less shape selective and produced more single ring aromatic products (BTX), but also produced high yields of polyaromatic hydrocarbon (PAH) products. Li et al. [24] studied several zeolite catalysts (ZSM-5, USY, β, SAPO-11, and ZSM-22) and reported that both the pore size and the acidity of the catalyst had very strong influence on the product yields. Gas yields increased and char yields decreased compared to thermal pyrolysis. SAPO-11 produced the highest yield of gases and the lowest yield of char because of its higher acidity and relatively larger pore size.

Investigation of the influence of basic catalysts such Al_2O_3, MgO, and $CaCO_3$ on WT pyrolysis showed that Al_2O_3 and $CaCO_3$ promoted gasification of the pyrolysis products whereas MgO promoted formation of liquid products [25]. Pyrolysis of WT using a mixture of basic and acidic catalysts (Al_2O_3 and SiO_2) produced almost equal amounts of aliphatic and aromatic compounds whereas Al_2O_3 alone produced a higher fraction of polar aromatics and lower amount of aliphatics. In contrast, the SiO_2 alone liquid products composition was the exact opposite of the Al_2O_3 [26]. Although these types of catalyst are relatively cheap compared to the zeolites, their acidity is rather weak, and they are not effective for cracking, isomerization, cyclization, or aromatization reactions. The basic catalysts are not as active for cracking C–C bonds compared to acidic catalysts, but are effective in hydrogenation, isomerization, and alkylation of heteroatomic compounds. MgO and $CaCO_3$ are the basic catalysts frequently used in WT pyrolysis to lower the sulfur

Table 1
Composition of different waste tires (wt%) [2].

Component	Car tires	Truck tires	Off road tires
Rubber/elastomers	47	45	47
Carbon black and silica	22.5	21	22
Metals	14	23.5	12
Textiles	5.5	1	10
Vulcanizer compounds	2.5	3	3
Additives	8.5	6.5	6
Total convertible organics	52.5	46	57
Total carbonaceous material	74.5	67	79

content of liquid products. Natural products such as olivine, dolomite, natural zeolites have also been investigated for WT pyrolysis and calcined olivine was shown to be more effective in sulfur removal [27]. $MgCl_2$ has been shown to be effective in sulfur removal from WT pyrolysis products [27].

Although there have been extensive catalytic pyrolysis studies of WT using both acidic and basic catalysts, there have not been many studies using red mud (RM) as a catalytic pyrolysis medium. RM is a by-product of the Bayer aluminum process, which involves digestion of bauxite in hot sodium hydroxide. The digestion of the ore results in a slurry of sodium aluminate solution and a caustic-insoluble residue, commonly referred to as RM. The chemical composition of RM varies worldwide and it consists of compounds originally present in the bauxite and those formed or introduced during the Bayer process. Typical composition of RM comprises of: Fe_2O_3 (30–60 wt%); Al_2O_3 (10–20 wt%); SiO_2 (3–50 wt%); Na_2O (2–10 wt%); CaO (2–8 wt%); TiO_2;(0.1–25 wt%). The RM is basic with a pH ranging from 10 to 13. Its properties such as high iron oxide content (Fe_2O_3), high surface area, sintering resistance, resistance to poisoning and low cost make it an attractive potential catalyst for many reactions [28,29]. It was demonstrated that such inexpensive catalyst as RM can improve economic feasibility of biomass pyrolysis [30–33]. Raw RM is very powdery when dried and very difficult to handle; however, formulated red mud (FRM) has catalytic properties and therefore has been investigated for biomass pyrolysis [34,35]. Modified RM has also been investigated for dechlorination of plastics, desulfurization, and many other applications [28]. Because RM is a mixture of various metal oxides and the above literature shows effectiveness of some metal oxides in WT pyrolysis, the goal of this research is to investigate FRM for the catalytic pyrolysis of WT for improving pyrolysis liquid properties as well as desulfurization of the pyrolysis liquids.

2. Materials and methods

2.1. Waste tire feedstock

The WT samples were supplied by Liberty Tire LLC (Salt Lake City, UT). The crumbs "as received" were about 30 mesh and were used as is for the pyrolysis studies. The WT samples were characterized for moisture and ultimate composition. Thermogravimetric analysis (TGA) was used to determine a suitable decomposition temperature for the fluidized bed pyrolysis studies. Thus, TA Instruments Q500 (TA Instruments, New Castle, DE) was used to pyrolyze the WT under nitrogen atmosphere. About 10 mg of WT was used and the heating rate was 10 °C/min and temperature ranged from 20 °C to 700 °C and nitrogen flow rate of 100 ml/min. The ultimate composition of the WT was determined using ThermoFisher Flash 2000 CHNS/O organic elemental analyzer (ThermoFisher Scientific. Inc, Waltham, MA).

2.2. Catalyst preparation and characterization

RM samples were obtained from an alumina processing company and formulated into a suitable form for fluidization and minimization of catalyst attrition as reported elsewhere [31,32,34,35]. The formulated red mud (FRM) catalysts were calcined at 600 °C for 6 h and sieved to particle size 180 μm $< d_p <$ 450 μm to avoid plugging of the hot gas filter used to remove tire char and fine catalyst particles.

The fresh (not used for pyrolysis), used, and regenerated catalysts were characterized using Brunauer-Emmette-Teller (BET) specific surface area method, as described in Jahromi and Agblevor [36–38]. Inductively coupled plasma/mass spectroscopy (ICP/MS)

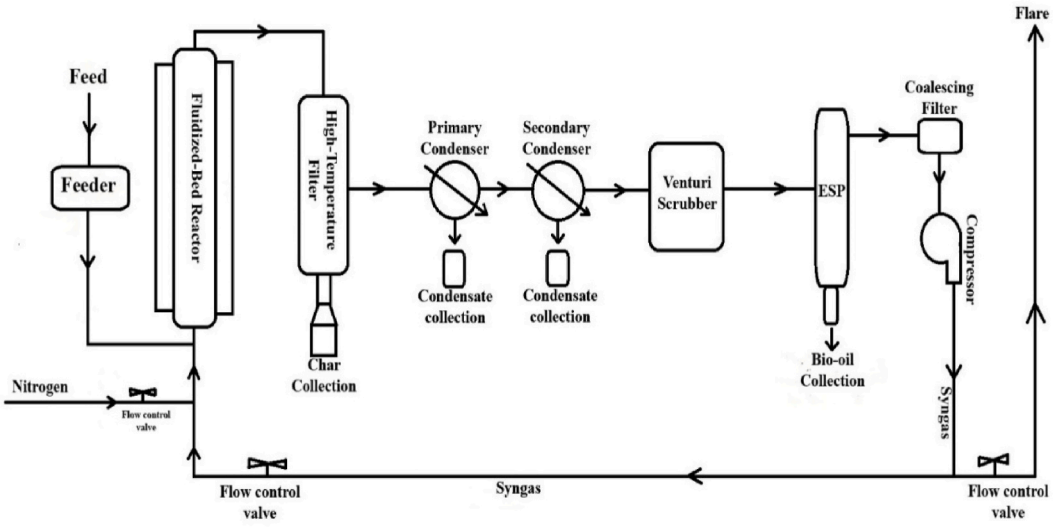

Fig. 1. Schematic diagram of fluidized bed reactor used for the pyrolysis of the waste tire.

was used to determine the elemental composition of the bulk fresh, used, and regenerated catalysts. The ICP/MS analysis was conducted by USU Analytical laboratory (Utah State University, Logan, UT). These analyses were complemented by X-ray diffraction (XRD) spectroscopic analysis. XRD analysis was conducted by Hoffman Hazen Laboratories (Golden, CO). All other analyses were conducted in-house at Utah State University, Logan, UT.

2.3. Catalytic pyrolysis of waste tires

Catalytic pyrolysis was conducted in a pilot scale bubbling fluidized bed pyrolysis reactor (Fig. 1) using FRM as the catalyst bed. Ground WT (30 mesh) were used as the feedstock. The details of the reactor description have been published previously and will not be repeated here [34]. The fluidized bed reactor was loaded with 1400 g FRM catalyst and heated to reaction temperature. The catalytic pyrolysis was conducted at 500 °C using N_2 as the initial fluidizing gas (2.0 scfm flow rate), which was gradually replaced with the non-condensable pyrolysis gases after compression and recycling. The moisture content of the WT crumbs was 1.5 wt% and the WT feed rate was 2 kg/h. The pyrolysis products were passed through a hot gas filter to separate tire char and fine catalysts from the vapors. The clean vapors were then sent through two shell and tube condensers and two coalescing filters for vapor condensation (Fig. 1). During the pyrolysis, oil samples were collected hourly from all the condensers and coalescing filters. Most runs were conducted for 5-, 10-, and 20 h time on stream (TOS) to determine the effect of pyrolysis on the catalyst activity and quality of the liquid product.

After each experiment, the catalyst and the tire char were collected from the hot gas filter and the reactor. The tire char was easily separated from the catalyst because after each run, the hematite (Fe_2O_3) in the FRM was converted to maghemite (γ-Fe_2O_3), which was magnetic and therefore easily separated from the tire char using a magnetic sieve. After tire char separation, the catalyst was regenerated in a muffle furnace at 650 °C overnight. The regenerated catalyst and ash from WT were separated by sieving the mixture to remove the ash. Any losses in catalyst due to attrition was replenished with fresh make-up catalyst. For very long runs (>20 h TOS) the catalyst lost its magnetic properties and therefore the used catalyst was regenerated directly by air combustion in a muffle furnace to recover the catalyst. At the end of each run, samples of catalyst were taken for characterization using methods described above.

The hourly oil samples collected from the coalescing filter were analyzed for viscosity, pH, density, Karl Fischer water content, and ultimate composition. Some of the oil samples were also hydrotreated to determine their stability using a nickel supported on red mud catalyst (Ni/RM) as reported in Jahromi and Agblevor [36–38].

2.4. Hydrotreatment of catalytic tire pyrolysis oils

The catalytic tire pyrolysis oil (CTPO) was hydrotreated using nickel supported on red mud (Ni/RM) catalyst at two different temperatures (350 °C and 400 °C) as described in Jahromi and Agblevor [36–38]. The reaction time was 30 min, the initial hydrogen pressure was 3.44 MPa (500 psi) and catalyst to oil ratio of 0.15. The hydrocarbon fraction was separated from the small aqueous phase by centrifugation and decantation. The organic fraction was characterized as described below. The gas product was analyzed using gas chromatographic methods described below.

2.5. Characterization of waste tires pyrolysis products

The WT pyrolysis products (gas, liquid, and tire char) were characterized using various techniques. The gaseous products were analyzed using SRI gas chromatograph equipped with flame ionization detector (FID) and thermal conductivity detector (TCD) (SRI Instruments, Torrance, CA). The pyrolysis gas components were quantified using standard gas samples purchased from Supelco® analytical products (Millipore Sigma, Burlington, MA). The tire char samples were analyzed for ultimate composition. The liquid products, CTPO, were extensively characterized using various methods described below.

The CTPO collected on hourly basis and the composite oils after a complete run were characterized for the various properties. The viscosities of the CTPOs were measured at 40 °C using SVM 3000 Staubinger viscometer (Anton Parr, Graz, Austria). The results were equivalent to viscosities determined by ASTM D445 method. The SVM 3000 Staubinger viscometer was also used to measure the densities of the oils. Calibrations were done prior to measurements with viscosity standard liquids. A Metrohm 701 KF Titrino (Metrohm Instruments, Riverview, FL) and a 703 titration stand setup were used for the Volumetric Karl Fischer titration. Hydranal® Composite 5 reagent was used. 50 ml of methanol was placed in the titration vessel and conditioned. About 60–100 mg of oil sample was loaded into a hypodermic plastic syringe and weighed. The sample was injected into the titration solvent and the syringe was weighed again. The water content was titrated volumetrically, and the resulting mass was recorded.

The elemental compositions of the CTPO were determined using ThermoFisher Flash 2000 CHNS/O organic elemental analyzer (ThermoFisher Scientific Inc, Waltham, MA). About 10 mg of sample was used for each analysis. The higher heating values (HHV) of the samples were determined using the IKA basic bomb calorimeter (IKA Works Inc, Wilmington, NC). Atmospheric batch distillation of the CTPO was carried out by Big West Oil LLC (Salt Lake City, UT) using ASTM D86 standard method to determine the distribution of various fuel fractions.

^{13}C NMR spectra were collected using a 500 MHz Agilent DD2 spectrometer with a 5 mm Agilent OneNMR Probe. A single pulse sequence used a 45° pulse on the carbon with ^{1}H decoupling during the acquisition (1 s). A 10 s recycle delay was used between pulses and 4000 scans were collected for each sample. The CTPO samples were prepared with deuterated chloroform (*d*-$CDCl_3$). The relaxant used was 0.05 M $Cr(acac)_3$. Inverse-gated decoupling protocol was used. The spectra were referenced to *d*-$CDCl_3$ (77 ppm) and integrated to obtain carbon mole fractions of the following functional groups: carbonyl (200–225 ppm), carboxyl (170–185 ppm),

phenolic (142–170 ppm), aromatic/olefinic (95–142 ppm), ether and/or alcohol (57–85), and paraffinic (0–52, exclusive of *d*- $CDCl_3$ peak region) carbons.

The gas chromatography/mass spectrometric (GC/MS) analysis of the CTPO was determined using a Shimadzu GC/MS system (Shimadzu Scientific Inc, Columbia, MD, USA) consisting of a GC-2010 connected to a GC/MS-QP2010S. The GC was equipped with a Phenomenex ZB-5HT Inferno capillary column (30 m × 0.32 mm x 0.25 μm). The carrier gas was high purity helium (99.99 %) at a flow rate of 2 mL/min. The GC injector temperature was set to 250 °C and the split ratio was 30. The temperature program of the GC oven was set as follows; initial heating at 15 °C/min from 25 °C to 250 °C, then ramped at 50 °C/min to 300 °C and finally held for 7.5 min. The ion source for the mass spectrometer was set at 200 °C and the solvent cut time was 1.5 min. The ionization energy was 70.0 eV and the analysis was performed in electron impact (EI) ionization mode over a scanning range (*m/z*) of 10–350 amu. The CTPO samples were dissolved in toluene (~0.02 g CTPO/g of toluene) prior to analysis. The injection volume was 3 μL. The individual peaks were integrated, and the corresponding compounds were identified. The reported chemicals had a 70 % match or higher and all peaks that had a lower match percentage were added to the unknown group.

3. Results and discussion

3.1. Thermogravimetric analysis of waste tires

The thermogravimetric analysis (TGA) of the WT was performed to enable a suitable temperature to be selected for the pyrolysis in the bubbling fluidized bed reactor. The TGA of the WT was performed at 10 °C/min from room temperature to 700 °C. The thermogram showed one minor and two major weight loss peaks (Fig. 2). The broad minor weight loss peak between 150 and 300 °C was attributed to the decomposition of plasticizers, additives, and petroleum oil added to the rubber during tire formulation to give it resilient thermo-mechanical properties [39]. The major weight loss peak between 300 and 400 °C with a maximum at 375 °C was attributed to natural rubber and other elastomeric components of the WT. Natural rubber, butadiene and styrene butadiene rubbers have been reported to have maximum decomposition peaks at 372–375 °C which agrees with the current data. The weight loss peak at 400–517 °C with a maximum at 444 °C was attributed to styrene butadiene (SBR, 372 and 429–460 °C), and butadiene rubber (BR, 372 and 460 °C)) components [39]. Our DTGA results are similar to those published in literature suggesting that our thermogram derived from the combination of the three types of rubber found in the WT. The TGA did not show any specific peak for the textile component of the WT, probably because it decomposed within the temperature range of the other rubbers/elastomers. The TGA data showed that the WT can be pyrolyzed between 400 and 500 °C, where most of the decomposition occurred. Thermal tire pyrolysis temperature as reported in literature ranges from 500 to 650 °C which agrees with the current data [6,8].

The pyrolysis residue from the TGA analysis was relatively high (34.4 wt%) because of the high carbon black, zinc oxide, and other additives such as clay content of the WT.

3.2. Characterization of fresh and used catalysts

The FRM catalyst used in these studies was from the same batch used for biomass pyrolysis reported by Agblevor et al. [34], which showed robustness towards deactivation from deposition of biomass inorganic components. In the biomass pyrolysis process, the catalyst was monitored for the deposition of inorganic components on its surface and its effect on the catalyst performance. It was observed that the deposition of K, Ca, P, and Mg from the biomass feedstock did not have any negative influence on the catalytic activity of the FRM. In particular, the K appeared to enhance the activity of the catalyst. Since the catalyst was robust towards deactivation when biomass inorganic components were deposited on it, it was hypothesized that it might be equally robust towards the

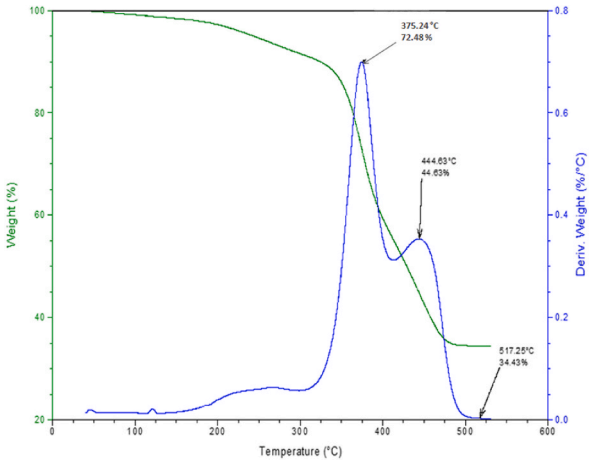

Fig. 2. TGA and DTGA of WT under nitrogen atmosphere at a heating rate of 10 °C/min.

deposition of WT inorganic compounds such as sulfur, zinc, and others. Thus, the goal of the WT *in situ* catalytic pyrolysis was to assess its robustness towards sulfur and other compounds used in tire formulation, to reduce the sulfur content of the liquid products, and improve oil quality. The FRM catalyst was used continuously for 20 h time-on-stream (TOS), and catalyst samples were taken at 0 h, 10 h, 20 h to assess the state of the catalyst using XRD analysis. The XRD spectra obtained at various time intervals during the *in situ* catalytic pyrolysis are shown in Fig. 3 and Table 2. The major compounds detected in the fresh catalyst (0 h TOS), were hematite (Fe_2O_3); sodalite ($Na_6(Al_6Si_6O_{24})_2NaF.xH_2O$); calcite ($CaCO_3$), anatase ($TiO_2$), Aluminum oxide ($Al_2O_3$), quartz ($SiO_2$) and trace amounts of rutile (TiO_2) as shown in Fig. 3a. The XRD spectrum of the catalysts sample after 10-h TOS is shown in Fig. 3b. The major differences between the two spectra were the disappearance of several peaks observed in Fig. 3a and the appearance of new peaks in Fig. 3b. The hematite peak in Fig. 3a disappeared and three new iron compounds ((maghemite (γ-Fe_2O_3), goethite ((FeO(OH)), pyrrhotite (FeS)) appeared in the spectrum. This clearly showed that the hematite underwent several chemical reactions with the WT decomposition products. This change in catalyst composition was quite different from those observed for the *in situ* catalytic pyrolysis of lignocellulosic biomass. In the case of lignocellulosic biomass using catalyst from the same batch, the major change observed was the conversion of the hematite to magnetite (Fe_3O_4) and goethite because of the reducing pyrolytic atmosphere of CO and H_2 produced from the decomposition of the biomass [32]. However, in the WT pyrolysis there was no magnetite peak, instead, maghemite was formed which was also magnetic. It is known that hematite can be converted into maghemite and magnetite under reducing conditions [40,41]. It is interesting to note that although the pyrolysis of both the lignocellulosic biomass and the WT were conducted under reducing atmosphere, the presence of sulfur compounds in the WT influenced the conversion pathway of hematite to magnetite and maghemite was formed instead.

The detection of FeS in the XRD spectrum showed that there was reactive adsorption desulfurization (RADS) of the WT pyrolysis products and subsequent reduction of sulfur content of CTPO as discussed in the next section. Some fraction of the hematite was also converted into goethite. Thus, the catalytic activity of the FRM was rather complex. The only other significant change in the catalyst composition was the disappearance of the rutile peak. It appeared that there was phase change under the reaction conditions to convert the rutile to anatase [42]. In contrast, the anatase, alumina, quartz, sodium, calcite peaks were all present similar to the fresh catalyst. It is interesting to note that calcite was still present in this spectrum, because one would have expected the calcite to react readily with the sulfur to form calcium sulfide and thus contribute to the desulfurization of the CTPO. It was also possible that there was some partial reaction between sulfur and calcite to form amorphous calcium sulfide which was not detected by the XRD.

The used catalyst spectrum after 20-h TOS (Fig. 3c–Table 2) showed more dramatic changes in its composition. This catalyst sample was weakly magnetic as was confirmed by the absence of maghemite and magnetite peaks in the XRD spectrum. The iron compounds were pyrrhotite (FeS), pyrrhotite (Fe_{1-x} S-11T (x = 0–0.12)), and goethite. The FeS peak was the most intense of the three peaks. The presence of the Fe_{1-x} S-11T peak implied further reaction of sulfur with the iron with attendant structural changes and reduction in the magnetism. Since neither magnetite nor maghemite peaks were present after 20-h TOS, the weak magnetism observed was attributed to the pyrrhotite which is known to be weakly magnetic [43].

There were two new peaks due to zinc compounds that were not present in the fresh FRM and 10-h TOS catalysts spectra (Fig. 3c–Table 2). These new peaks were identified as wurtzite-2H (ZnS) and sphalerite (ZnS), that were attributed to the deposition of zinc oxide from the WT on the catalyst surface which then reacted with either metal sulfides, sulfur, or H_2S in the CTPO vapors. It is known that metal sulfides react with ZnO to form ZnS as a desulfurization mechanism for hydrocarbon fuels. It appears that a similar reaction took place during the WT pyrolysis because no ZnS was detected until after the formation of FeS [44,45]. These reactions also contributed to the desulfurization of the CTPO. Alumina, quartz, sodalite, anatase, and rutile were all present as usual suggesting that these oxides did not react with the sulfur compounds in the WT pyrolysis products. There was no calcite peak in this spectrum which suggested that the calcite reacted to form some amorphous calcium compounds that were not detected in the XRD diffractogram.

After 20-h TOS, the catalyst was regenerated in air at 650 °C overnight and sieved to remove the ash. The regenerated catalyst was analyzed using the XRD and the spectrum is shown in Fig. 3d. The regenerated catalyst spectrum was similar to the fresh catalyst spectrum (compare Fig. 3a and d) except the presence of four new peaks that were not present in the fresh catalyst. The new peaks were

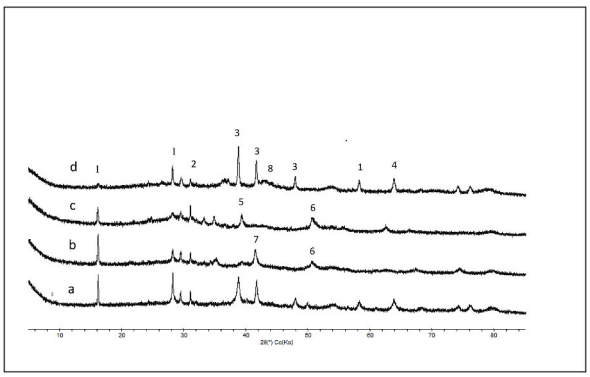

Fig. 3. XRD spectra of catalysts after various times-on-stream (TOS): a) fresh catalyst (0 h TOS); b) 10 h TOS; c) 20 h TOS; d) regenerated catalyst. 1 = $Na_6(Al_6Si_6O_{24})_2NaF{\cdot}xH_2O$; 2 = SiO_2; 3 = Fe_2O_3; 4 = TiO_2; 5 = $Fe_{1-x}S$; 6 = FeS; 7 = Fe_3O_4; 8 = ZnO.

Table 2
Major compounds detected in the XRD spectra of FRM catalyst at various time on stream (x = detected; TOS = time on stream)).

Compounds	Formula	Fresh (0 h TOS)	10 h TOS	20 h TOS	Regenerated
Quartz	SiO_2	x	x	x	x
Sodalite	$Na_6(Al_6Si_6O_{24})_2NaF.xH_2O$	x	x	x	x
Hematite	Fe_2O_3	x			x
Calcite	$CaCO_3$	x	x		
Anatase	TiO_2	x	x	x	
Alumina	Al_2O_3	x	x	x	x
Rutile	TiO_2	x		x	
Maghemite	ɣ-Fe_2O_3		x		
Goethite	FeO(OH)		x	x	
Pyrolithite	FeS		x	x	
Pyrrhotite	Fe_{1-x}S-11T (x = 0–0.12)		x	x	
Wurtzite-2H	ZnS			x	
Sphalerite	ZnS			x	
Dolomite	$CaMg(CO_3)_2$				x
Anhydrite	$CaSO_4$				x
Sodium sulfate	Na_2SO_4				x
Zincite	ZnO				x

identified as $CaSO_4$, Na_2SO_4, $CaMg(CO_3)_2$, and ZnO (Table 2). The presence of the $CaSO_4$ was attributed to the reaction of calcite with the sulfur compounds from the WT pyrolysis vapors to form calcium sulfide which although was not detected in the non-regenerated catalyst became visible as calcium sulfate because of the oxidation of the sulfide to sulfate in air during the regeneration [46,47]. The Na_2SO_4 was also a product of the reaction of NaOH with the sulfur compounds generated from the pyrolytic reaction of the WT, which were then converted into sulfate during the regeneration process. The dolomite $CaMg(CO_3)_2$ was attributed to the reaction of the calcite with magnesium additive in the WT during the regeneration process. The other significant change in the regenerated spectrum was the lower intensity of the sodalite ($Na_6(Al_6Si_6O_{24})_2NaF$) peak which could be attributed to conversion to amorphous compounds. All the iron compounds produced during the pyrolysis such as FeS, Fe_{1-x}S-11T, and FeO(OH) were converted into hematite during the regeneration in air and the catalyst was subsequently non-magnetic.

The presence of ZnO in the spectrum was attributed to the oxidation of wurtzite and sphalerite in air during the regeneration process. Alumina and quartz peaks were still present like the original fresh catalyst. Another significant difference between the regenerated catalyst and the fresh catalyst was the absence of the anatase and rutile peaks in the spectrum which suggested that probably amorphous phase was formed after the regeneration of the catalyst.

From the FRM spectra it was clear that sulfur removal from the CTPO was through several reactive adsorption processes. These reactions were due to the hematite, calcite, and sodium hydroxide contents of the FRM catalyst. However, after the regeneration the contribution of the calcite and sodium hydroxide were lost because they were converted into sulfates which were unreactive. However, the deposition of zinc oxide on the catalyst surface had a positive effect on the desulfurization process because it reacted to produce zinc sulfide compounds. The activity of the catalyst after regeneration was not lost because hematite and zinc oxide were now the active compounds for sulfur removal. The more interesting aspect of this catalyst was the increase in zinc oxide content with TOS which compensated for any loss of desulfurization activity from the loss of calcite and NaOH.

After the regeneration of the used catalyst, sulfur compounds did not completely disappear but rather some sulfur was retained as sodium and calcium sulfates, which were stable at the catalyst regeneration temperatures. This finding agrees with the ICP/MS analyses of the regenerated catalyst which showed 2.71 wt% sulfur content (discussed below). The regenerated catalyst was reused for catalytic pyrolysis, and it was very active and reduced the sulfur content of the CTPO as expected (data not reported).

The XRD analyses of the fresh and used catalysts were corroborated with ICP/MS analysis at various stages of catalyst time on stream. Fig. 4 shows the trends in deposition of sulfur and zinc on the catalyst. Sulfur concentration increased with TOS but appeared to

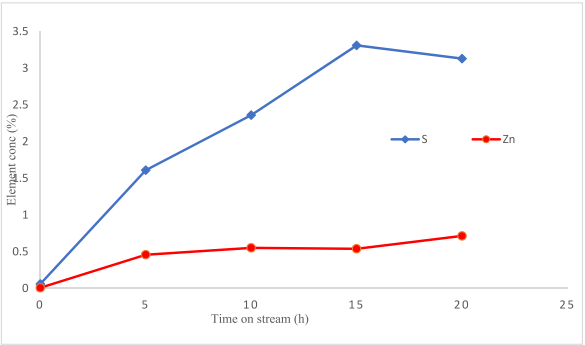

Fig. 4. Changes in element concentration on catalysts during pyrolysis time on stream.

plateau after 15-h probably because all the active catalyst sites were saturated. The initial concentration of sulfur in the fresh catalyst was 0.06 wt% (600 ppm), but this increased to 3.31 wt% (33100 ppm) after 15-h TOS. The sulfur deposition on the catalyst surface emanated from its release from the pyrolysis products of WT which underwent reactive adsorption on the catalyst surface. Since the pyrolysis conditions were reductive, it was postulated that sulfur was released as H_2S which was adsorbed on the catalyst surface and subsequently reacted initially with hematite forming pyrrhotite (FeS) and also with sodium hydroxide and calcite components of the catalyst.

The zinc content of the catalyst also increased with increased TOS, but this was less rapid compared to the sulfur (Fig. 4). The initial concentration of zinc in the catalyst was 8.6 ppm but this increased to 7139 ppm after 20-h TOS. No elemental zinc peak was detected in the XRD, but wurtzite and sphalerite which are reaction products of zinc oxide and metal sulfides were detected. The wurtzite and sphalerite peaks were not observed in the XRD until 20-h TOS and no elemental zinc peak was detected in the XRD whereas the ICP/MS data showed zinc deposition throughout the TOS (Fig. 4). This apparent contradiction was probably because the ZnO was not reduced to elemental zinc and the zinc compounds initially deposited on the catalyst surface were amorphous and not reflected in the XRD spectra. The reaction of ZnO with sulfur started when there appeared to be saturation of the active sites of hematite (Fig. 4). Furthermore, it appeared that the ZnO did not react directly with the sulfur compounds but rather reacted with FeS and $Fe_{1-x}S$ as reported by Han et al. [48].

The pyrolysis gas mixture contained CO, CO_2, H_2 and low molecular weight hydrocarbons, but these did not appear to reduce the ZnO to Zn. It is known that CO_2 suppresses the reduction of ZnO to Zn because any zinc formed from the reduction rapidly reacts with the CO_2 to form fresh ZnO [49].

3.3. 3. Waste tire catalytic pyrolysis products

The ground WT material was free-flowing and easy to feed into the reactor without melting in the screw feeder junction with the hot reactor. The ultimate analysis of the WT (79.31 wt% C, 7.45 wt% H, 0.55 wt% N, 2.23 wt% S, 10.46 wt% O and 7.19 wt% ash) showed composition similar to those reported in literature [6,8]. The ash content of the WT was relatively high compared to lignocellulosic biomass feedstocks, but it was similar to those reported in literature for WT [6,8]. The carbon content of the WT was also very high because of the carbon black and the elastomer content. The oxygen content determined by difference was relatively low compared to lignocellulosic biomass feedstocks.

The *in situ* catalytic pyrolysis experiments were conducted at different TOS to assess catalyst activity, regenerability, life, and quality of oil. Thus, experiments were conducted for 5-, 10-, and 20-h TOS. The CTPO vapor condensation was quite different from lignocellulosic pyrolysis oils condensation in that for lignocellulosic pyrolysis oils, about 40 % of the pyrolysis oils condensed in the electrostatic precipitator (ESP) because of aerosol formation in the fluidized bed reactor. However, for the CTPO vapor, there was very little condensation in the ESP unit, instead the vapors by-passed the ESP and condensed in the coalescing filter placed after the ESP unit. Subsequently, the reactor configuration was changed by addition of an extra coalescing filter unit before the ESP. This new configuration with coalescing filters before and after the ESP was effective in condensing the CTPO vapors. The CTPO collected in the coalescing filters contained very little water (<1 %). The shell and tube condensers collected most pyrolytic water and the coalescing filter collected majority of the clean CTPO. The yields of the pyrolysis products are shown in Table 3. The CTPO liquid yields were lower than those reported in literature because most published tire pyrolysis systems used thermal pyrolysis, which normally produces higher yield than catalytic pyrolysis systems. Catalytic pyrolysis systems tend to produce higher gas yields than thermal pyrolysis, but the quality of the oils is usually superior to thermal pyrolysis oils for lignocellulosic biomass because of lower oxygen content.

During the catalytic pyrolysis process, oil samples were collected hourly for viscosity measurements. The variation in the viscosities of the biomass catalytic pyrolysis oils with TOS has been shown to be a function of the catalyst activity [31,34]. In general, the viscosity of lignocellulosic biomass catalytic pyrolysis oils increases as the catalyst activity decreases. The variation in the viscosity of CTPO with TOS is shown in Fig. 5. The viscosities of CTPO samples decreased with TOS which contrasted with lignocellulosic biomass catalytic pyrolysis oils using catalyst from the same batch preparation. The viscosities of compounds depend on carbon chain length and the degree of branching. Straight chain hydrocarbons are more viscous than branched chain hydrocarbons [50–53] and low molecular weight compounds have lower viscosity than the higher molecular weight compounds. Thus, we can surmise that the decrease in

Table 3
Distribution of waste tire catalytic pyrolysis products.

Catalyst	TOS (h)	Total liquids (wt%)	Organic liquid (wt%)	Pyrolytic water (wt%)	Char (wt%)	Gases (wt%)
Sand	n/a	37.59	35.46	2.13	39.0	23.41
FRM (5 h TOS)	5	36.32	31.13	5.19	39.78	23.90
FRM (10 h TOS)	10	35.33	34.33	1.00	40.33	23.62
FRM (20 h TOS)	20	37.50	35.25	2.25	40.95	21.55
Average pyrolysis gas composition (mol%)						
H_2	44.52					
CO	2.50					
CO_2	5.33					
CH_4	10.83					
C_2–C_4	36.80					
Total	99.98					

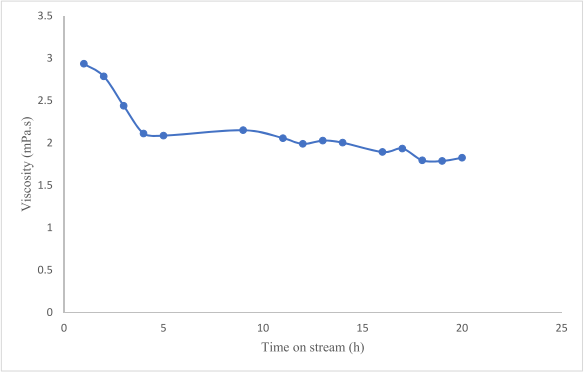

Fig. 5. Variation of CTPO viscosity with time on stream during WT catalytic pyrolysis.

viscosity of the CTPO with TOS was probably due to cracking of higher molecular weight compounds to lower molecular weight compounds promoted by new compounds formed on the catalyst surface with increased TOS. It has been reported that FeS catalyzes the reduction in viscosity of heavy oils [54] and since FeS was formed on the surface of the catalyst during the pyrolysis of WT, it is plausible to assume that it catalyzed the reduction in viscosity of the CTPO with increase in TOS as shown in Fig. 5. It has also been reported that the cleavage of the C–S bond in high molecular weight components of heavy oils results in decrease in oil viscosity, which probably occurred in the CTPO [55]. It has been reported that the reduction in sulfur content of waste tire pyrolysis oils correlated with the reduction in viscosity of the oils [52], which agrees with our data.

The total liquid yield (organic fraction + pyrolytic water) was relatively low compared to lignocellulosic biomass liquid yield and the yield did not vary much whether sand or FRM was used as the pyrolysis medium (Table 4). The total liquid yields were within the range for CTPO reported in literature [18–21]. The pyrolytic water was very low, but as expected the char yield was very high because of the carbon black and other tire additives in the WT. The gas yields did not vary much with TOS nor the pyrolysis medium but was only slightly higher than those produced in lignocellulosic biomass catalytic pyrolysis.

The carbon content of the char was similar to the WT but there was significant difference in the hydrogen content because the char was predominantly carbon black that was used in formulating the tires (Table 4). After pyrolysis, the carbon content of the char should have been higher because of loss of the volatile component of the WT and accumulation of carbon black and pyrolysis char. The low hydrogen and carbon contents appeared to be due to contamination of the char by the catalyst which will increase the ash content.

The sulfur content of the pyrolysis char was very high showing that the char retained a large fraction of the sulfur during the pyrolysis process which agrees with published literature [56]. However, some of the tire char sulfur could also be due to contamination with catalyst which was shown in Fig. 4 to have accumulated a substantial amount of sulfur during the pyrolysis process. This catalyst contamination will also affect the hydrogen and carbon contents of the char. The WT had a high ash content as expected because of various additives added during the vulcanization and tire formulation. No ash content was determined for the catalytic pyrolysis char because of interference from catalyst particles that stuck to the char.

3.3.1. Waste tire catalytic pyrolysis gas products

The gaseous products composition shown in Table 3 were analyzed using gas chromatograph. The dominant gases were hydrogen and C_2–C_4 hydrocarbons which agrees with published literature [18–21]. The CO and CO_2 contents were relatively low compared to lignocellulosic non-condensable pyrolysis gases because of the low oxygen content of the WT. Methane production was modest probably because there was not much cracking of the long chain hydrocarbons.

3.3.2. Characterization of catalytic tire pyrolysis oil

The CTPO was characterized for ultimate composition, higher heating value (HHV), sulfur content, chemical functional groups, and batch atmospheric distillation. The ultimate analysis of the CTPOs (Table 4) showed a considerable reduction in sulfur content relative to the WT. The initial WT had a sulfur content of 2.23 wt% which if all were retained in the oil would amount to 6.37 wt% for sand

Table 4
Ultimate composition of waste tires and pyrolysis products

Elements	WT	Tire char	CTPO	Sand pyrolysis oil
C **(wt%)**	79.31	79.21	87.42	87.23
H **(wt%)**	7.45	1.41	10.40	10.01
N **(wt%)**	0.55	0.31	1.41	0.03
S **(wt%)**	2.23	2.61	0.38	0.80
O **(wt%)**	10.46	16.46	0.38	1.93
Ash **(wt%)**	7.19	22.0	nd	nd
H/C	1.13	0.21	1.42	1.37

pyrolysis oil and 6.37–7.16 wt% for the CTPO. However, the sand pyrolysis oil sulfur content was 0.8 wt% while that for the CTPO was 0.38 wt%. Thus, a considerable amount of sulfur was removed through both thermal and catalytic pyrolysis processes. The sand pyrolysis oil sulfur was similar to those reported in literature, but the CTPO had a much lower sulfur content because of the desulfurization activity of the catalyst. The sulfur content of CTPO was slightly lower than those reported for catalytic pyrolysis using various desulfurization additives and others using two state reactors combined with various additives. This showed that the FRM method is superior to those reported in literature [19,57,58].

In addition to the ultimate analysis of the of the composite CTPO shown in Table 4, the hourly CTPO samples collected during each run as a function of TOS were also analyzed for sulfur content (Fig. 6). The sulfur content of the CTPO decreased with TOS because of the increased catalytic activity from the deposition of zinc oxide from the pyrolysis of WT which complemented the activities of hematite, NaOH, and $CaCO_3$, the main desulfurization agents in the FRM. With increase in TOS, the active catalyst sites responsible for the reactive adsorption desulfurization (RADS) gradually increased because of the Zn/ZnO deposition on the catalyst surface. Thus, there was decrease in the sulfur content of the CTPO even after 20-h TOS. Furthermore, since the process was RADS, improved desulfurization could be obtained by increasing the catalyst to WT ratio. In Fig. 6, if the catalyst loading is increased and there was catalysts regeneration every 10-h TOS, CTPO with less than 0.3 wt% sulfur could be produced in a continuous process. This type of oil will be suitable for marine diesel applications where the International Marine Organization (IMO) sulfur limit is 0.5 wt%.

3.3.3. ^{13}C NMR analysis of catalytic tire pyrolysis oils

The CTPOs were analyzed for functional composition using ^{13}C NMR spectroscopy. A typical ^{13}C NMR spectrum is shown in Fig. 7. The spectrum was composed of mostly aliphatic and aromatic hydrocarbons. The oxygenated compounds content was extremely low (4.5 %) and there were neither carbonyl compounds nor carboxylic acids (see Table 5). The low oxygenated compounds content was corroborated by the CHNOS analysis data (Table 4) which showed very low oxygen content (0.38 wt%). Thus, the catalyst was very effective in deoxygenation compared to sand which had five times more oxygen (1.93 wt%) than the CTPO.

3.3.4. GC/MS analysis of tire pyrolysis oils

The CTPO was analyzed qualitatively with GC/MS to assess the overall composition of the oils and to relate the chemical functional groups detected in the ^{13}C NMR to specific compounds. The qualitative GC/MS analysis of the CTPO is shown in Table S1 (Supplementary data). The peak assignment was done using NIST database of compounds. The quality of each compound identification had a spectral match greater than 70 %. About 78 % of the CTPO compounds were identified and about 22 % were assigned to unknown compounds. The compound with the highest relative concentration was DL-limonene, which constituted 25.73 % of the total chromatographic area. The presence of DL-limonene in the CTPO was not surprising since this compound has been reported by several researchers in the past and various attempts have been made to isolate it from the mixture [23,59,60]. However, most of those reports were based on non-catalytic pyrolysis studies. In those reports, DL-limonene was the dominant compound in the tire pyrolysis oils. The other compounds detected in the CTPO were at lower relative concentrations with most of them 5 % or lower. Most of the compounds identified were aliphatic and the unknowns were probably aromatic and alkenes, which agrees with the ^{13}C NMR data discussed above. Other than the DL-limonene, the concentration of other compounds was too low to be worthy of isolation for other applications. This implies that the CTPO will be most suitable for low-carbon fuel applications because some fraction derives from biomass sources.

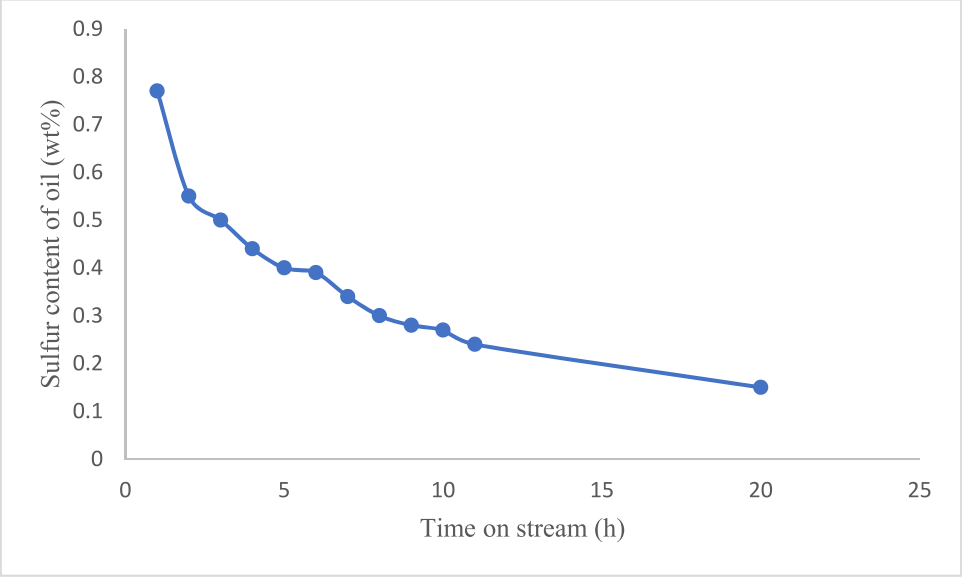

Fig. 6. Variation in sulfur content of CTPO with TOS during WT catalytic pyrolysis.

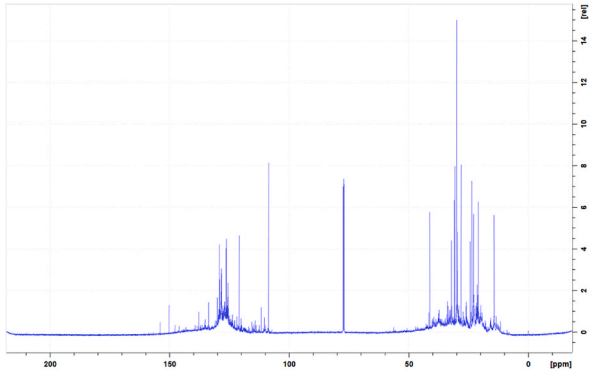

Fig. 7. ^{13}C NMR spectrum of CTPO oil sample in $CDCl_3$; the deuterated chloroform solvent peak is shown at 77 ppm.

Table 5
Relative concentration of chemical functional groups in CTPO^{13}C NMR

Chemical functional groups	Integrated peak area (%)
Saturated aliphatics (0–50 ppm)	56.8
Aliphatic chains with heteroatoms (O and/or N) and methoxy group (50–110 ppm)	4.5
Olefins and aromatics (110–160 ppm)	38.7
Esters, Carboxylic acids (160–180 ppm)	0
Ketones/Aldehydes (180–220 ppm)	0
Total	100

3.3.5. 5. Batch atmospheric distillation catalytic tire pyrolysis oils

Since the ^{13}C NMR and GC/MS analyses suggested that the potential application of the CTPO could be low-carbon fuel, some samples were characterized using the ASTM D86 batch atmospheric distillation method. The atmospheric distillation plot of the CTPO is shown in Fig. 8. The gasoline fraction was relatively low (10 wt%) while the diesel fraction was highest (58.1 wt%). The heavy oil fraction was 31.9 wt% while the Jet A fuel fraction was 27.4 wt% (Table 6). This fuel could therefore find application as International Marine organization (IMO) diesel fuel because of its high diesel and heavy oil fractions and its relatively low sulfur content (0.38 wt% or 3800 ppm) which is below the minimum required for IMO marine diesel fuel (5000 ppm or 0.5 wt%). The CTPO could also be potentially used as Jet A fuel. The fuel will however not qualify for road transportation because of its relatively high sulfur content.

3.4. Hydrotreatment of the catalytic tire pyrolysis oil

The batch atmospheric distillation studies showed that the CTPO had a relatively high heavy oil fraction and very low gasoline fraction and therefore the oil was hydrotreated. After hydrotreatment there was a significant change in the atmospheric distillation curve of the liquid fractions as shown in Fig. 8. The hydrotreatment doubled the gasoline fraction and reduced the heavy oil and diesel fractions (Table 6). The lower heavy oil fraction and a reduced amount of diesel fraction were attributed to cracking of both the heavy oil and diesel fractions to lighter compounds which increased the gasoline and Jet A fuel fractions. The Jet A fuel fraction increased from 27.4 wt% to 35.3 wt% after the hydrotreatment. The quality of the fuel also improved after the hydrotreatment as shown in Table 6. The density of the fuel was reduced from 0.91 g/cm^3 to 0.79 g/cm^3 and the viscosity of the fuel decreased from 1.79 to 1.23 mPa s. The higher heating value (HHV) of the fuel increased from 42.66 to 45.67 MJ/kg. The H/C ratio increased with hydrotreatment suggesting that the product contained fewer aromatic compounds. As can be seen from Table 7, the properties of the liquid product were strongly influenced by the hydrotreating temperature. At higher hydrotreating temperature the quality of the fuel improved due to cracking of heavy oil and diesel factions resulting in lower viscosities and densities. The HHV also improved with temperature because of improved deoxygenation and the sulfur content also decreased with increased hydrotreating temperature. However, gas, coke, and aqueous phase yields increased with increased hydrotreating temperature (Table 7).

The gas composition from the hydrotreated samples were similar to those reported for catalytic biomass pyrolysis oils and guaiacol under similar hydrotreating conditions [36–38]. The dominant compound was methane because of conversion of CO and CO_2 over the nickel catalyst to produce methane. All other gas components except C_4H_{10} and C_5H_{12} increased with increased reaction temperature because of increased cracking and methanation reactions.

4. Conclusions

The catalytic pyrolysis of waste tires (WT) using formulated red mud (FRM) catalyst showed that sulfur from the WT was removed through two mechanisms: retention in the char products and reactive adsorption desulfurization by the FRM catalyst. The hematite, NaOH, $CaCO_3$ from the FRM reacted with the sulfur compounds to desulfurize the catalytic pyrolysis vapors. As the reaction proceeded

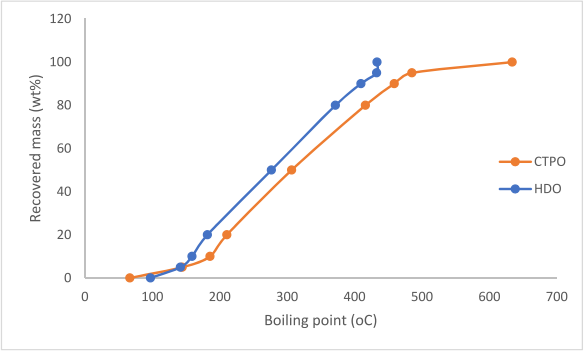

Fig. 8. Batch atmospheric distillation curves of tire pyrolysis oils.

Table 6
Batch atmospheric distillation fractions of CTPO

Boiling temperature range (°C)	Fuel type	CTPO Fraction recovered (wt%)	Hydrotreated CTPO Fraction recovered (wt%)
IBP-184	gasoline	10	22.7
184–344	Diesel	58.1	48.9
152–256	Jet A	27.4	35.3
>344	Heavy oil	31.9	28.4

Table 7
CTPO properties before and after hydrotreatment (HYD = hydrotreated)

	CTPO	HYD oil-350 °C	HYD oil-400 °C
H_2 consumption **(g H_2/g oil)**	–	0.0053	0.0086
Density **(g/cm^3)**	0.91	0.81	0.79
Viscosity **(mPa.s)**	1.79	1.58	1.23
Organic liquid **(wt%)**	–	90.36	85.43
Aqueous liquid **(wt%)**	–	3.82	4.37
Gas **(wt%)**	–	4.77	8.32
Coke **(wt%)**	–	1.04	1.87
HHV **(MJ/kg)**	42.66	43.78	45.67
API gravity	21.1	nd	29.6
Ultimate composition of hydrotreated liquid products			
C **(wt%)**	87.42	nd	87.90
H **(wt%)**	10.40	nd	11.73
N **(wt%)**	1.41	nd	0.61
S **(wt%)**	0.38	nd	0.03
O **(wt%)**	0.39		0.08
H/C	1.43		1.60
Composition hydrotreated gas products (mol%)			
CO	–	5.85	6.31
CO_2	–	11.83	10.73
CH_4	–	67.12	69.45
C_2H_6	–	6.56	7.11
C_3H_8	–	4.48	5.13
C_4H_{10}	–	4.07	1.21
Total		99.91	99.94

nd = not determined.

with time on stream, zinc oxide from the WT was deposited on the catalyst surface which also reacted with the sulfur compounds. The major sulfur compounds formed were FeS, FeS_{1-X}, ZnS, CaS, Na_2S. Continuous pyrolysis was carried out for 20 h TOS before the catalyst was partially deactivated. After regeneration, the activity of the catalyst was restored but some of the sulfur adsorption components such as $CaCO_3$ and NaOH were converted into $CaSO_4$, $NaSO_4$ and $CaMg(CO_3)_2$ which were lost but ZnO was deposited on the catalyst to compensate for the lost components. The CTPO had relatively low sulfur content and very good fuel properties and could potentially be used as marine diesel or Jet A fuels. The higher heating value (HHV) was similar to that of conventional diesel fuel. The CTPO also had a relatively high *DL*-limonene, aliphatic, and low aromatic compounds contents.

Data availability

Data will be made publicly available.

CRediT authorship contribution statement

Foster A. Agblevor: Writing – review & editing, Writing – original draft, Supervision, Project administration, Methodology, Investigation, Conceptualization. **Oleksandr Hietsoi:** Writing – review & editing. **Hossein Jahromi:** Writing – review & editing, Investigation. **Hamza Abdellaoui:** Writing – review & editing.

Declaration of competing interest

The authors declare that they have no known competing financial interests or personal relationships that could have appeared to influence the work reported in this paper.

Acknowledgement

The authors acknowledge funding from the Utah Science Technology and Research program, Utah, USA.

Appendix A. Supplementary data

Supplementary data to this article can be found online at https://doi.org/10.1016/j.heliyon.2024.e33121.

References

[1] https://www.ustires.org/sites/default/files/2019%20USTMA%20Scrap%20Tire%20Management%20Summary%20Report.pdf.
[2] A. Fazil, D. Rodrigue, Recycling waster tire into ground tire rubber (GTR)/rubber compounds: a review, J. Compos. Sci. 4 (2020) 103, https://doi.org/10.3390/jcs4030103.
[3] Scrap Tires: Handbook on recycling applications and management for U.S. and Mexico, 2010. United States Environmental Protection Agency, Office of Resource Conservation and Recovery, Washington DC, *EPA530-R-10-010*, www.epa.gov/waste.
[4] C. Roy, A. Chaala, H. Darmstadt, B. de Caumia, H. Pakdel, J. Yang, Conversion of used tires to carbon black and oil by pyrolysis, Rubber Recycling (2005) 429–467.
[5] M. Juma, Z. Koreňová, J. Markoš, J. Annus, L. Jelemenský, Pyrolysis and combustion of scrap tire, Petroleum & Coal 48 (2006) 15–26.
[6] P.T. Williams, Pyrolysis of waste tyres: a review, Waste Manag. 33 (2013) 1714–1728.
[7] N. Antoniou, A. Zabaniotou, Features of an efficient and environmentally attractive used tyres pyrolysis with energy and material recovery, Renew. Sustain. Energy Rev. 20 (2013) 539–558.
[8] J.D. Martinez, N. Puy, R. Murillo, T. Garcia, M.V. Navarro, A.M. Mastral, Waste tyre pyrolysis – a review, Renew. Sustain. Energy Rev. 23 (2013) 179–213.
[9] A. Alsaleh, M.L. Sattler, Waste tire pyrolysis: Influential parameters and product properties, Curr Sustain. Renew. Energy Rep. 1 (2014) 129–135.
[10] J.I. Osayi, S. Iyuke, S.E. Ogbeide, Biocrude production through pyrolysis of used tyres, J. Catalysts (2014) 386371/1–386371/9.
[11] P. Parthasarathy, H.S. Choi, H.C. Park, J.G. Hwang, H.S. Yoo, B.-K. Lee, M. Upadhyay, Influence of process conditions on product yield of waste tyre pyrolysis - a review, Korean J. Chem. Eng. 33 (2016) 2268–2286.
[12] S.T. Kumaravel, A. Murugesan, A. Kumaravel, Tyre pyrolysis oil as an alternative fuel for diesel engines – a review, Renew. Sustain. Energy Rev. 60 (2016) 678–1685.
[13] A. Quek, R. Balasubramanian, Liquefaction of waste tires by pyrolysis for oil and chemicals – a review, J. Anal. Appl. Pyrolysis 101 (2013) 1–16.
[14] I. Hita, M. Arabiourrutia, M. Olazar, J. Bilbao, J.M. Arandes, P. Castaño, Opportunities and barriers for producing high quality fuels from the pyrolysis of scrap tires, Renewable Sustainable Energy Rev. 56 (2016) 745–759.
[15] J.D. Martinez, N. Puy, R. Murillo, T. Garcia, M.V. Navarro, A.M. Mastral, Waste tyre pyrolysis–A review, Renewable Sustainable Energy Reviews 23 (2013) 179–213.
[16] Q. Shi, J. Wu, Review on sulfur compounds in petroleum and its products: state of the art and perspectives, Energy & Fuels 18 (2021) 14445–14461.
[17] A. Demirbas, H. Alidrisi, M.A. Balubaid, API gravity, sulfur content, and desulfurization of crude oil, Pet. Sci. Technol. 33 (2015) 93–101.
[18] M. Arabiourrutia, G. Lopez, M. Artetexe, J. Bilbao, M. Olazar, Waste tyre volarization by catalytic pyrolysis- A review, Renewable Sustainable Energy Rev. 129 (2020) 109932.
[19] G.-G. Choi, S.-J. Oh, J.-S. Kim, Clean pyrolysis oil from a continuous two-stage pyrolysis of scrap tires using in situ and ex-situ desulfurization, Energy 141 (2017) 2234–2241.
[20] P.T. Williams, A.J. Brindle, Catalytic pyrolysis of tyres: influence of catalyst temperature, Fuel 81 (2002) 2425–2434.
[21] Y. Kar, Catalytic pyrolysis of car tire waste using expanded perlite, Waste Manag. 31 (2011) 1772–1782.
[22] X. Zhang, T. Wang, L. Ma, J. Chang, Vacuum pyrolysis of waste tires with basic additives, Waste Manag. 28 (2008) 2301–2310.
[23] M. Olazar, R. Aguado, M. Arabiourrutia, G. Lopez, A. Barona, J. Bilbao, Catalyst effect on the composition of tire pyrolysis products, Energy & Fuels 22 (2008) 2909–2916.
[24] W. Li, C. Huang, D. Li, et al., Derived oil production by catalytic pyrolysis of scrap tires, Chin. J. Catal. 37 (2016) 526–532.
[25] S. Kordoghli, M. Paraschiv, R. Kuncser, M. Tazerout, F. Zagrouba, Catalysts' influence on thermochemical decomposition of waste tires, Environ. Prog. Sustain. Energy 36 (2017) 1560–1567.
[26] J. Shah, M.R. Jan, F. Mabood, Recovery of value-added products from the catalytic pyrolysis of waste tyre, Energy Convers. Manag. 50 (2009) 991–994.
[27] A. Hooshmand Ahoor, N. Zandi-Atashbar, Fuel production based on catalytic pyrolysis of waste tires as an optimized model, Energy Convers. Manag. 87 (2014) 653–669.
[28] S. Sushil, V.S. Batra, Catalytic applications of red mud, an aluminum industry waste: a review, Appl. Catal. 81 (2008) 64–77.
[29] S. Wang, H.M. Ang, M.O. Tade, Novel applications of red mud as coagulant, adsorbent and catalyst for environmentally benign processes, Chemosphere 72 (2008) 1621–1635.

[30] S. Kelkara, C.M. Saffrona, K. Andreassia, Z. Li, A. Murkuteb, D.J. Millerb, T.J. Pinnavaiad, R.M. Kriegele, A survey of catalysts for aromatics from fast pyrolysis of biomass, Appl. Catal. B Environ. 174 (2015) 85–95.

[31] F.A. Agblevor, D.C. Elliott, D.M. Santosa, M.V. Olarte, S.D. Burton, M. Swita, S.H. Beis, K. Christian, B. Sargent, Red mud catalytic pyrolysis of pinyon juniper and single stage hydrotreatment of oils, Energy Fuels 30 (2016) 7947–7958.

[32] B.K. Yathavan, F.A. Agblevor, Catalytic pyrolysis of pinyon−juniper using red mud and HZSM-5, Energy Fuels 27 (2013) 6858–6865.

[33] J.R. Kastner, R. Hilten, J. Weber, A.R. McFarlane, J.S. Hargreaves, V.S. Batrac, Continuous catalytic upgrading of fast pyrolysis oil using iron oxides in red mud, RSC Adv. 5 (2015) 29375–29385.

[34] F.A. Agblevor, H. Wang, S. Beis, K. Christian, A. Slade, O. Hietsoi, D.M. Santosa, Reformulated red mud: a robust catalyst for in situ catalytic pyrolysis of biomass, Energy & Fuels 34 (2020) 3272–3283.

[35] D.M. Santosa, C. Zhu, F.A. Agblevor, B. Maddi, B.Q. Roberts, I.V. Kutnyakov, S.J. Lee, H. Wang, In situ catalytic fast pyrolysis using red mud catalyst: impact of catalytic fast pyrolysis temperature and biomass feedstocks, ACS Sustainable Chem. Eng. 8 (2020) 5156–5164.

[36] H. Jahromi, F.A. Agblevor, Hydrodeoxygenation of aqueous-phase pyrolysis oil to liquid hydrocarbons using multifunctional nickel catalyst, Ind. Eng. Chem. Res. 57 (2018) 13257–13258.

[37] H. Jahromi, F.A. Agblevor, Hydrotreating of guaiacol: a comparative study of red mud supported nickel and commercial Ni/SiO_2-Al_2O_3 catalysts, Appl. Catal. Gen. 558 (2018) 109–121.

[38] H. Jahromi, F.A. Agblevor, Hydrodeoxygenation of pinyon juniper catalytic pyrolysis oil using red mud supported nickel catalyst, Appl. Catal. B Environ. 236 (2018) 1–12.

[39] D.Y.C. Leung, C.L. Wang, Kinetic study of scrap tyre pyrolysis and combustion, J. Anal. Appl. Pyrol. 45 (1998) 153–169.

[40] A. Aharoni, E.H. Frei, M. Scheiber, Some properties of Υ-Fe_2O_3 obtained by hydrogen reduction of α-Fe_2O_3, J. Phys. Chem. Solids 23 (1962) 545–554.

[41] W.K. Jozwiak, E. Kaczmarek, T.P. Maniecki, W. Ignaczak, W. Maniukiewicz, Reduction behavior of iron oxides in hydrogen and carbon monoxide atmospheres, Appl. Catal., A 326 (2007) 17–27.

[42] S. Bagheri, N.M. Julkapli, S.B.A. Hamid, Titanium dioxide as catalyst support in heterogeneous catalysis, Sci. World J 2014 (2014) 21, https://doi.org/10.1155/2014/727496.

[43] S. Atak, M.S. Celik, G. Onal, Innovations in Mineral and Coal Processing, Taylor and Francis, Jan 1, 1998, 1998. ISBN 9058090132.

[44] S. Jin, Q. Yue, T. Meng, H. Zhang, N. Jiang, M. Jin, R. Zhang, Ultra -deep desulfurization via reactive adsorption on nickel and zinc species supported on activated carbon, J. Porous Mater. 24 (2017) 1697–1704.

[45] L. Huang, G. Wang, et al., In situ XAS study on the mechanism of reactive adsorption desulfurization of oil product over Ni/ZnO, Appl. Catal., B 106 (2011) 26–38.

[46] Y. Ninomiya, A. Sato, A.P. Watkinson, Oxidation of Calcium Sulfide in Fluidized Bed Combustion/generation Conditions, 1995 287963. *CONF-950*522, ISBN 0791813053; OSTI Identifier.

[47] N.H. Davies, K.M. Laughlin, A.N. Hayhurst, The oxidation of calcium sulfate at the temperature of fluidized bed combustors, Symposium (International) on Combustion 25 (1) (1994) 211–218, 1994.

[48] J. Han, W. Liu, T. Zhang, K. Xue, W. Li, F. Jiao, W. Qin, Mechanism study on the sulfidation of ZnO with sulfur and iron oxide at high temperature, Sci. Rep. 7 (2017) 42536, https://doi.org/10.1038/srep42536(2017).

[49] E. Sasaoka, S. Hirano, S. Kasaoka, Y. Sakata, Stability of Zinc oxide high-temperature desulfurization sorbents for reduction, Energy & Fuels 8 (1994) 763–769.

[50] G. Knothe, K.R. Steidley, Kinematic viscosity of biodiesel fuel components and related compounds. Influence of compound structure and comparison to petrodiesel fuel components, Fuel 84 (9) (2005) 1059–1065.

[51] A.J. Folayan, P.A.L. Anawe, A.E. Aladejare, A.O. Ayeni, Experimental investigation of the effect of fatty acids configuration, chain length, branching and degree of unsaturation on biodiesel fuel properties obtained from lauric oils, high-oleic and high-linoleic vegetable oil biomass, Energy Rep. 5 (2019) 793–806.

[52] J.B. Omwoyo, R.K. Kimilu, J.M. Onyari, Effects of temperature and catalytic reduction of sulfur content on kinematic viscosity and specific gravity of tire pyrolysis oil, Chem. Eng. Comm. 210 (1) (2023) 129–136.

[53] https://www.britannica.com/science/hydrocarbon/Physical-properties.

[54] Z. Zhou, M. Slaný, E. Kuzielov, W. Zhang, L. Ma, S. Dong, J. Zhang, G. Chen, Influence of reservoir minerals and ethanol on catalytic aquathermolysis of heavy oil, Fuel 307 (2022) 121871.

[55] I.I. Mukhamatdinov, A.R. Khaidarova, K.D. Zaripova, R.E. Mukhamatdinova, S.A. Sitnov, A. Vakhin, The composition and structure of ultra-dispersed mixed oxide (II, III) particles and their influence on in-situ conversion of heavy oil, Catalysts 10 (1) (2020) 114, https://doi.org/10.3390/catal10010114.

[56] H. Hu, Y. Fang, H. Liu, R. Yu, G. Luo, W. Liu, A. Li, H. Yao, The fate of sulfur during rapid pyrolysis of scrap tires, Chemosphere 97 (2014) 102–107.

[57] H. Aydın, C. Ilkılıç, Optimization of fuel production from waste vehicle tires by pyrolysis and resembling diesel fuel by various desulfurization methods, Fuel 102 (2012) 605–612.

[58] F. Campuzano, A.G.A. Jameel, W. Zhang, A.-H. Emwas, A.F. Agudelo, Fuel and chemical properties of waste tire pyrolysis oil derived from a continuous twin-auger reactor, Energy Fuels 34 (2020) 12688–12702.

[59] J. Alvarez, G. Lopez, M. Amutio, N.M. Mkhize, B. Danon, P. van der Gryp, J.F. Gorgens, J. Bilbao, M. Olazar, Evaluation of the properties of tyre pyrolysis oils obtained in a conical spouted bed reactor, Energy 128 (2017) 463–474.

[60] K. Januszewicz, P. Kazimierski, W. Kosakowski, W.M. Lewandowski, Tyre pyrolysis for obtaining limonene, Materials 13 (2020) 1359, https://doi.org/10.3390/ma13061359.